Neurochemistry International 129 (2019) 104470

Contents lists available at ScienceDirect

Neurochemistry International

journal homepage: www.elsevier.com/locate/neuint

$App^{NL-G-F/NL-G-F}$ mice overall do not show impaired motivation, but cored amyloid plaques in the striatum are inversely correlated with motivation

Takuya Hamaguchi[a,*], Iku Tsutsui-Kimura[b,1], Masaru Mimura[a,b], Takashi Saito[c], Takaomi C. Saido[c], Kenji F. Tanaka[b]

[a] Center for Kampo Medicine, Keio University School of Medicine, 35 Shinanomachi, Shinjuku-ku, Tokyo, 160-8582, Japan
[b] Department of Neuropsychiatry, Keio University School of Medicine, 35 Shinanomachi, Shinjuku-ku, Tokyo, 160-8582, Japan
[c] Laboratory for Proteolytic Neuroscience, RIKEN Center for Brain Science, 2-1 Hirosawa, Wako-shi, Saitama, 351-0198, Japan

ARTICLE INFO

Keywords:
Alzheimer
Apathy
Operant
Lever
Break point
Dopamine transporter

ABSTRACT

Apathy is clinically defined as lack of motivation. Apathy is a frequent symptom in patients with Alzheimer's disease (AD). It is unclear whether amyloid β (Aβ) pathology is associated with apathy. To address this question, we employed the $App^{NL-G-F/NL-G-F}$ mouse, an Aβ deposition-bearing mouse without neurofibrillary tangles and neuronal cell death throughout the lifespan and used a progressive-ratio (PR) task to monitor instrumental motivation between the ages of 16 and 39 weeks. In the PR task, the number of lever presses to receive one reward increases and the number of active lever presses in the final trial a mouse completes represents a break point, which is an index of motivation. During the observation period, $App^{NL-G-F/NL-G-F}$ mice overall did not show impaired motivation. However, $App^{NL-G-F/NL-G-F}$ mice showed a dispersion of the break point at 39 weeks of age within the group. Therefore, we examined the association between the degree of the break point and Aβ pathology; the number of cored amyloid plaques in the striatum was inversely correlated with the degree of motivation. Furthermore, we measured the dopamine transporter (DAT) levels in the subcortical tissues including the striatum using western blot analysis and showed that $App^{NL-G-F/NL-G-F}$ mice have lower DAT levels than do C57BL/6J mice. Although we could not directly determine the effect of core amyloid plaques on the DAT, the results of this study suggest a pathway through which cored amyloid plaques damage the DAT and cause impaired motivation. These results will draw attention to cored amyloid plaques and will aid researchers searching for new strategies that are effective for the prevention and treatment of impaired motivation.

1. Introduction

The pathology of Alzheimer's disease (AD) is characterized by deposition of amyloid β (Aβ) and formation of neurofibrillary tangles (NFTs), which are aggregates of phosphorylated tau (p-tau) protein. Aβ deposition is considered to begin approximately 30 years before AD onset, followed by p-tau accumulation for approximately 10 years before AD onset (Sasaguri et al., 2017). Various neuropsychiatric symptoms are connected with these long-lasting histopathological features in patients with AD. Among those symptoms, the most frequent is apathy with an overall prevalence of 49%, followed by depression, aggression, anxiety, and sleep disorder in this order (Zhao et al., 2016).

Apathy is clinically defined as lack of motivation (Marin, 1990). Apathy in patients with dementia leads to decreased activities of daily living and impedes their rehabilitation (Sondell et al., 2018; Williams, 2005). Apathy is also seen in patients with mild cognitive impairment (MCI) before AD onset, and it is known that the comorbidity of apathy with MCI accelerates AD progression (Robert et al., 2006; Teng et al., 2007). Therefore, an understanding of apathy pathophysiology in AD/MCI is necessary to evaluate a patient's prognosis and may help to explore new treatment options.

Recently, it has been reported that in patients with AD the severity of apathy positively correlates with the degree of prefrontal Aβ deposition (Mori et al., 2014). Although this study did not control for the effects of NFTs on apathy, it suggested that Aβ deposition per se results in apathy. To address the question whether Aβ deposition per se causes apathy, we employed the unique $App^{NL-G-F/NL-G-F}$ mouse model (Saito et al., 2014) in which Aβ accumulates without overexpression of APP,

* Corresponding author. .
E-mail addresses: takuya_hamaguchi@keio.jp (T. Hamaguchi), ikimura@fas.harvard.edu (I. Tsutsui-Kimura), mimura@keio.jp (M. Mimura), takashi.saito.aa@riken.jp (T. Saito), takaomi.saido@riken.jp (T.C. Saido), kftanaka@keio.jp (K.F. Tanaka).
[1] Present address:Center for Brain Science, Department of Molecular and Cellular Biology, Harvard University, Cambridge, Massachusetts 02138, USA.

https://doi.org/10.1016/j.neuint.2019.104470
Received 20 October 2018; Received in revised form 13 May 2019; Accepted 15 May 2019
Available online 16 May 2019
0197-0186/

List of abbreviations

Aβ	amyloid β
AD	Alzheimer's disease
Cg	cingulated cortex
CPu	striatum
DAT	dopamine transporter
GAPDH	glyceraldehyde-3-phosphate dehydrogenase
GP	globus pallidus
FR	fixed ratio
MCI	mild cognitive impairment
mPFC	medial prefrontal cortex
NFT	neurofibrillary tangle
PBS	phosphate buffered saline
PR	progressive ratio
ROI	region of interest
TBS	tris buffered saline
VTA	ventral tegmental area

leading to artificial phenotypes; Aβ deposition starts at 2 months of age and plaques accumulate over time, while NFT formation and neuronal cell death do not occur throughout the lifespan of these animals. The characteristics of the $App^{NL\text{-}G\text{-}F/NL\text{-}G\text{-}F}$ mouse model allowed us to examine the influence of Aβ deposition itself on motivation.

Some behavioral changes have been reported in the $App^{NL\text{-}G\text{-}F/NL\text{-}G\text{-}F}$ mouse model. In the Y-maze test, $App^{NL\text{-}G\text{-}F/NL\text{-}G\text{-}F}$ mice showed memory impairment at 6 months of age (Saito et al., 2014). In a study utilizing the IntelliCage system, $App^{NL\text{-}G\text{-}F/NL\text{-}G\text{-}F}$ mice showed cognitive impairments such as difficulty in flexible learning, decreased attention performance, and increased impulsiveness at 13–14 months of age (Masuda et al., 2016). Furthermore, Mehla et al. revealed age-dependent memory impairments with maximum impairment at the age of 12 months in the Morris water maze, fear conditioning tests, and the object recognition test (Mehla et al., 2019).

Apathy is also defined as a quantitative reduction of self-generated and voluntary goal-directed behaviors (Levy and Dubois, 2006). According to this definition, apathy (or apathy-like behavior in animals) can be quantified in animals by measuring goal-directed behavior. In the current study, we monitored the change in goal-directed behavior utilizing the food-oriented lever-press task to address instrumental motivation in $App^{NL\text{-}G\text{-}F/NL\text{-}G\text{-}F}$ mice for 6 months.

Finally, we analyzed the influence of Aβ pathology on motivation. Aβ pathology is classified into two types, cored and non-cored amyloid plaques, according to the pattern of β-amyloid distribution (Griffin et al., 1995). Qualitative differences in Aβ pathology have been reported. In brain tissues from patients with AD, cored amyloid plaques are associated with inflammatory cells, while non-cored amyloid plaques are not associated with neuronal death (D'Andrea and Nagele, 2010). However, the relevance of qualitative differences in Aβ pathology for motivation has not been explored yet. Therefore, we investigated its relevance by staining amyloid plaques and cored amyloid plaques in $App^{NL\text{-}G\text{-}F/NL\text{-}G\text{-}F}$ mice.

2. Materials and methods

2.1. Animal model

All animal procedures were conducted in accordance with the National Institutes of Health Guide for the Care and Use of Laboratory Animals and approved by the Animal Research Committee of Keio University School of Medicine. The $App^{NL\text{-}G\text{-}F/NL\text{-}G\text{-}F}$ mouse model comprises a knock-in mouse in which gene mutations are inserted into exons 16 and 17 (amyloid β cording region) of the mouse App gene. In addition to humanization of the mouse amyloid β sequence, a triple mutation with Swedish mutation (NL), Arctic mutation (G), and Beyreuther/Iberian mutation (F), known as mutations in familial AD, are introduced (Saito et al., 2014). $App^{NL\text{-}G\text{-}F/NL\text{-}G\text{-}F}$ mice and C57BL/6J mice were maintained at 24 °C with a 12 h light/dark cycle.

Eleven male $App^{NL\text{-}G\text{-}F/NL\text{-}G\text{-}F}$ mice (RIKEN BioResource Center #06344, Saitama, Japan) and eight male C57BL/6J mice (Oriental Yeast Co., Ltd., Tokyo, Japan), all 7 weeks old, were used for the behavioral and histological studies. Behavioral testing was conducted during the light phase of this cycle (8:00 a.m. to 8:00 p.m.). Mice were fed with normal chow (MF, Oriental Yeast Co., Ltd.) and housed individually with ad libitum water access in each home cage for the first week (from 7 to 8 weeks of age). After the first week, food intake was restricted to the amount of 2.3 g on the day before every session of the operant training and testing.

Five $App^{NL\text{-}G\text{-}F/NL\text{-}G\text{-}F}$ mice and five C57BL/6J mice at 9 months of age were used for the western blot analysis.

2.2. Apparatus

Two-lever operant test chambers (Med Associates Inc., St. Albans, VT, USA) enclosed in sound-attenuating compartments were used. The reinforcers were sucrose pellets (20 mg each, dustless precision pellets; Bio-Serv, Frenchtown, NJ, USA), which were delivered to a feeder arranged between the two levers. A Siemens Nixdorf computer programmed in MED-PC (Med Associates Inc.) controlled the experiment and collected data.

2.3. Behavioral procedures

Operant training and testing sessions were conducted according to previously reported methods (Fig. 1A, Hamaguchi et al., 2017). Briefly, during operant training sessions, which were conducted six times per week, the session was initiated at a fixed ratio (FR)-1 reinforcement schedule, whereby a single active lever press elicited the delivery of a food pellet. Following a session in which ≥50 trials were attained in 60 min, the session schedule was increased to FR-2. Similar to the FR-1 to FR-2 transition, the schedule was increased to FR-3 and then to a progressive ratio (PR) reinforcement schedule. For the PR reinforcement schedule, the response ratio schedule was calculated using the following formula: $5e^{R\times0.2} - 5$, where R is the number of food rewards already earned plus 1 (Fig. 1B, Richardson and Roberts, 1996). The final ratio completed (the number of active lever presses in the final trial a mouse completed/how long a mouse effortfully pressed the active lever to receive one reward) represented the break point ($5e^{(R-1)\times0.2} - 5$, eq. 1). This was used as an index of instrumental motivation. Following a session in which ≥10 trials were attained and the mean time spent to complete the required number of lever presses was < 10 s, the schedule was changed to the PR reinforcement schedule with one limitation; if the number of active lever presses did not reach the number necessary for food rewards within 10 min after the beginning of the session, the session was terminated. When the number of rewards earned in a session deviated by ≤ 10% for 3 consecutive days, learning was considered completed in the operant training session. If the learning was not completed before 16 weeks of age, the mouse was excluded from further experiments. During operant test sessions, we applied the "long-term operant test method" where the PR reinforcement schedule was conducted twice a week until the age of 39 weeks.

2.4. Indices of the operant test

The indices in the PR reinforcement schedule were as follows. The break point (see eq. 1) was recognized as an index of instrumental motivation, the %Accuracy [active lever-press numbers/(active and

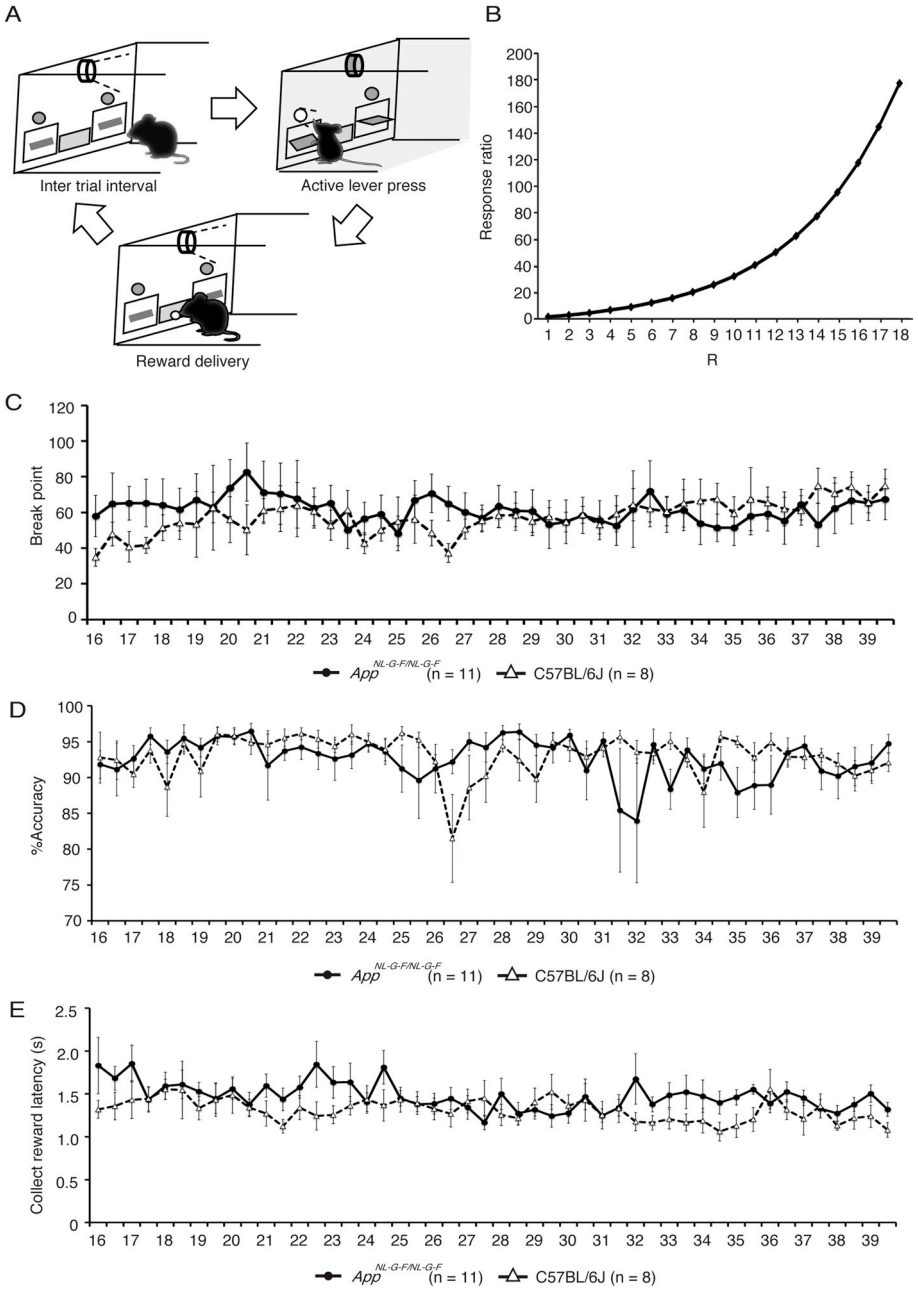

Fig. 1. Results of progressive ratio (PR) reinforcement in the food-oriented lever-press task in $App^{NL\text{-}G\text{-}F/NL\text{-}G\text{-}F}$ and C57BL/6J mice. PR experiments were conducted twice per week during the testing session period. **A,** the image shows the flow of the food-oriented lever-press task. **B,** the graph shows the response ratio calculated by the formula $5e^{R\times 0.2} - 5$, where R is the number of food rewards already earned plus 1. **C,** the graph shows the value of the break point as an index of motivation. The break point was nearly stable in the testing sessions of both groups. **D,** the accuracy to press the reward lever was not affected and was almost over 90% in $App^{NL\text{-}G\text{-}F/NL\text{-}G\text{-}F}$ mice. **E,** the collect reward latency was stable in both groups indicating that the appetite of the mice did not change.

inactive lever-press numbers) × 100] was considered an index of cognitive function, and the collect reward latency was recognized as an index of appetite.

2.5. Histology

After the behavioral testing, the mice were deeply anesthetized and transcardially perfused with 4% paraformaldehyde. Brains were removed, post-fixed in 4% PFA overnight, and cryoprotected in a 20% sucrose solution for 1 day. Then, brains were frozen in 2-methylbutane (FUJIFILM Wako Pure Chemical Corp., Osaka, Japan), chilled with liquid nitrogen, and sliced with a cryostat into 30 μm-thick sections and mounted on silane-treated microscope slides (Matsunami Glass Ind., Ltd., Osaka, Japan). For amyloid plaque immunostaining, we performed antigen retrieval to the slides by heating (121 °C for 5 min) in immunoactive solution (Matsunami Glass Ind., Ltd.), used peroxidase-conjugated (Dojindo Molecular Technologies, Inc. #LK11, Kumamoto, Japan) anti-human amyloid β (N) (82E1) mouse IgG monoclonal antibody (1:100) (Immuno-Biological Laboratories Co., Ltd. #10323, Gunma, Japan) specific for the N-terminal region of Aβ, and amplified the signal with tyramide (PerkinElmer, Inc., Waltham, MA, USA).

For cored amyloid plaque staining, brain sections were briefly rinsed in H_2O and steeped in 70% EtOH for 5 min. The sections were incubated in 1% (w/v) Thioflavin S (Sigma-Aldrich Co. LLC., St. Louis, MI, USA) 70% EtOH solution at room temperature for 30 min. The sections were rinsed in 70% EtOH four times for 5 min and in phosphate

buffered saline (PBS) for 2 min once. Then, the sections were incubated in Hoechst nuclear counterstain (Thermo Fisher Scientific Inc., Waltham, MA, USA) for 15 min and rinsed in PBS three times. Sections were cover-slipped with ProLong Gold (Thermo Fisher Scientific Inc.). Stained slides were scanned with a NanoZoomer-XR C12000 (Hamamatsu Photonics K.K., Shizuoka, Japan).

There is a technical issue with Thioflavin S becoming partially detached from the amyloid β sheets due to the heating (121 °C for 5 min) needed for antigen retrieval for the 82E1 antibody staining. Therefore, we performed double staining with the 82E1 antibody and Thioflavin S only in order to demonstrate morphological differences between cored and non-cored amyloid plaques. When we measured the %Area of amyloid plaques or the number of cored amyloid plaques, we stained slides separately with the 82E1 antibody or Thioflavin S.

2.6. Western blot analysis

Mice were deeply anesthetized and transcardially perfused with PBS, and the brains were rapidly removed. The subcortical brain area including the striatum (CPu) was dissected and flash frozen in liquid nitrogen. Samples were added into lysis buffer (50 mM Tris (pH 7.6), 1% Triton-X, Protease Inhibitor Tablet (Roche Life Science #11836145001, Penzberg, Germany), and Protease Inhibitor Cocktail Solutions I and II (Fujifilm Wako Pure Chemical Corp. #167–24381 and #160–24371, Osaka, Japan)) in tris buffered saline (TBS) on ice. Samples were crushed using Multi-Beads Shocker (Yasui-kiki, Osaka, Japan) and incubated in the lysis buffer for 1 h on ice. Samples were spun at 15,000 rpm for 15 min at 4 °C. The supernatants were analyzed with the BCA Protein Assay Kit (Thermo Fisher Scientific Inc. #23227) to assess protein concentration. The supernatants were added to 2-mercaptoethanol and diluted with the lysis buffer to 15 μg protein/20 μl, boiled for 3 min at 100 °C, and loaded onto 5–20% e-PAGEL (ATTO Corp., Tokyo, Japan). Gels were electrophoresed at 20 mA for 1.5 h, and proteins were transferred to a polyvinylidene difluoride membrane and a nitrocellulose membrane for 1 h at 2 mA/mm^2. The nitrocellulose membrane was boiled for 3 min at 100 °C. Membranes were blocked with 2% ECL Prime Blocking Agent (GE Healthcare Life Sciences #RPN418V, Buckinghamshire, UK) in TBS with Tween (TBS-T). Membranes were probed for the dopamine transporter (DAT, 1:1,000, Frontier Institute co., ltd. #DAT-Rb-Af1800, Hokkaido, Japan) or horseradish peroxidase conjugated glyceraldehyde-3-phosphate dehydrogenase (GAPDH, 1:150,000, Proteintech Group, Inc. #HRP-60004, Chicago, IL, USA) and incubated overnight at 4 °C. Membranes were washed with TBS-T and then probed with the ECL horseradish peroxidase conjugated anti-rabbit IgG (1:2,000, GE Healthcare Life Sciences, #NA9340V). Amersham ECL Select (GE Healthcare Life Sciences) was used for visualization.

2.7. Data analysis

The obtained data in the histological analysis were analyzed with ImageJ (NIH, Bethesda, MD, USA). In the analysis using ImageJ, the appropriate algorithms were applied to binarize the images of amyloid plaques: the IsoData algorithm in the cingulated cortex (Cg), the medial prefrontal cortex (mPFC), and the ventral tegmental area (VTA) and the Intermodes algorithm in the CPu and the globus pallidus (GP). To calculate the number of cored amyloid plaques, images were created by subtraction between the image of Thioflavin S and Hoechst and the appropriate thresholds were applied to binarize the images: the threshold of 45–255 in the mPFC, the Cg, and the CPu and the threshold of 60–255 in the GP and the VTA.

The membranes used in the western blot analysis were scanned with LAS4000 (Fujifilm, Tokyo, Japan), and protein densities were analyzed using the Multi Gauge software (Fujifilm).

Two-factor repeated measures analysis of variance (ANOVA), Levene's test, stepwise multiple regression analysis, and Student's *t*-test were performed using SPSS Statistics 23.0 (IBM Corp., Armonk, NY, USA). In the analysis of two-factor repeated measures ANOVA and stepwise multiple regression analysis, missing values were stored by series average. In the analysis of two-factor repeated measures ANOVA, a Greenhouse–Geisser correction was used when the assumption of sphericity was violated. Data are shown with the mean and standard error of the mean. Values of $p < 0.05$ were considered statistically significant. In the box plots, the distribution in the samples is displayed based on the five-number summary: minimum, first quartile, median, third quartile, and maximum.

3. Results

3.1. Overall, $App^{NL\text{-}G\text{-}F/NL\text{-}G\text{-}F}$ mice showed stable motivation in the testing sessions

To address food-seeking motivation in mice, we used the PR task in which the amount of effort to obtain one palatable pellet progressively increases trial by trial. The animals eventually stopped obtaining the reward, and we measured the number of lever presses in the last successful trial as a break point (see eq. 1), an index of instrumental motivation. The animals started the training sessions of operant conditioning at the age of 8 weeks and finished their training before the age of 16 weeks. The number of sessions spent on operant conditioning did not differ between the two genotypes (data not shown, $p = 0.310$) and all mice included in this study completed the training before the age of 16 weeks.

We monitored instrumental motivation from 16 to 39 weeks of age with long-term testing using a modified version of the PR task in which the animals perform test sessions twice per week (Hamaguchi et al., 2017). Comparing the two groups, we found that $App^{NL\text{-}G\text{-}F/NL\text{-}G\text{-}F}$ mice did not show decline of the break point (week: $F_{4.65,\ 78.97} = 0.74$, $p = 0.586$; group: $F_{1,\ 17} = 0.11$, $p = 0.748$; week × group interaction: $F_{4.65,\ 78.97} = 0.93$, $p = 0.465$, Fig. 1C), suggesting that the continuous increase of Aβ deposition for 6 months did not impair instrumental motivation.

We also addressed cognitive function. In our operant experiment, the apparatus had two levers, levers providing and not providing reward, and the animals learned this association. The accuracy to press the reward lever (%Accuracy) was used as an index of cognitive function. The parameter %Accuracy was stable in both groups from 16 to 39 weeks of age (week: $F_{4.11,\ 69.89} = 1.17$, $p = 0.332$; group: $F_{1,\ 17} = 0.05$, $p = 0.825$; week × group interaction: $F_{4.11,\ 69.89} = 1.25$, $p = 0.298$; Fig. 1D), indicating that cognitive function was not affected in $App^{NL\text{-}G\text{-}F/NL\text{-}G\text{-}F}$ mice up to 39 weeks of age.

A change in appetite can be a confounding factor of food-seeking motivation. We measured the collect reward latency, which signifies the time from reward delivery to feed acquisition. If the appetite increases, the collect reward latency decreases, and vice versa. The values of the collect reward latency were stable in both groups from 16 to 39 weeks of age (week: $F_{8.47,\ 143.97} = 1.19$, $p = 0.305$; group: $F_{1,\ 17} = 2.19$, $p = 0.157$; week × group interaction: $F_{8.47,\ 143.97} = 1.09$, $p = 0.373$; Fig. 1E), supporting that the appetite did not change during the operant test sessions.

3.2. An increased number of cored amyloid plaques in the CPu coincided with impaired motivation

The continuous increase of Aβ deposition for 6 months appeared not to impair instrumental motivation in $App^{NL\text{-}G\text{-}F/NL\text{-}G\text{-}F}$ mice. When we

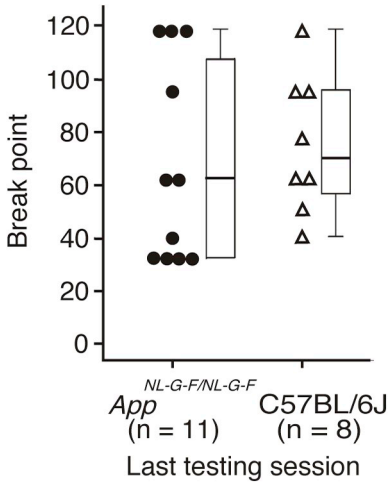

Fig. 2. The comparison of the degree of dispersion of the break point in $App^{NL\text{-}G\text{-}F/NL\text{-}G\text{-}F}$ and C57BL/6J mice at 39 weeks of age. The scatter plot shows the value of the break point of each mouse, and the box plot shows the degree of dispersion in each genotype. Larger dispersion of the break point was found in $App^{NL\text{-}G\text{-}F/NL\text{-}G\text{-}F}$ mice than in C57BL/6J mice.

plotted the value of the break point at 39 weeks of age on scatter plots and box plots, we could see larger dispersion of the break point among the $App^{NL\text{-}G\text{-}F/NL\text{-}G\text{-}F}$ mice than among the C57BL/6J mice (Fig. 2, $p = 0.120$ in Levene's test). Therefore, as a group sub analysis, we examined whether the degree of the break point in the last testing session was associated with the degree of Aβ deposition.

We selected the Cg (approximately bregma +1.78 mm), the mPFC (prelimbic cortex and infralimbic cortex, approximately bregma +1.78 mm), the CPu (approximately bregma +0.50 mm), the GP (approximately bregma −0.46 mm), and the VTA (VTA and parabrachial pigmented nucleus of the VTA, approximately bregma −2.92 mm) as the regions of interest (ROIs) (Fig. 3A), since these areas regulate the reward system in humans and mice. Dysfunction of the Cg and mPFC are well known to mediate apathy in patients with AD (Benoit et al., 2002; Craig et al., 1996; Holthoff et al., 2005; Kang et al., 2012; Marshall et al., 2007). Dysfunction in the CPu is reported to relate to apathy in patients with AD (David et al., 2008) and patients with frontotemporal dementia (Eslinger et al., 2012). Dysfunction in the VTA is also related to apathy in patients with AD and frontotemporal dementia (Schroeter et al., 2011). Although an association between dysfunction of the GP and apathy in patients with dementia has not been reported, some reports have shown that the GP regulates motivated behavior in humans (Caravaggio et al., 2018; Saga et al., 2017).

We stained brain sections with the 82E1 antibody and Thioflavin S and showed two typical types of amyloid plaques (Fig. 3B): cored amyloid plaques (82E1 (+), Thioflavin S (+)) and non-cored amyloid plaques (82E1 (+), Thioflavin S (−)). We measured the %Area of amyloid plaques where the 82E1 antibody was positive (Fig. 3C) and the number of cored amyloid plaques per mm^2 where Thioflavin S was positive (Fig. 3D) in the ROIs and show the results in Table 1. Then, stepwise multiple regression analysis was applied to predict the break point at 39 weeks of age based on amyloid plaques in the ROIs and cored amyloid plaques in the ROIs. The regression equation was significant ($F_{1,9} = 9.65$, $p = 0.013$), with an R^2 of 0.517. The predicted break point at 39 weeks of age was equal to 192.173–2.873 (cored amyloid plaques in the CPu), where cored amyloid plaques in the CPu are measured in number per mm^2 (Fig. 4). The break point at 39 weeks of age in $App^{NL\text{-}G\text{-}F/NL\text{-}G\text{-}F}$ mice decreased by 2.873 for each number per mm^2 of cored amyloid plaques in the CPu. Cored amyloid plaques in the CPu were a significant predictor of the break point at 39 weeks of age, and an increased number of cored amyloid plaques coincided with impaired motivation among the 11 $App^{NL\text{-}G\text{-}F/NL\text{-}G\text{-}F}$ mice at 39 weeks of age.

3.3. There were significantly lower DAT levels in the subcortical brain tissues including the CPu in $App^{NL\text{-}G\text{-}F/NL\text{-}G\text{-}F}$ than in C57BL/6J mice

A single-photon emission computed tomography study using the ^{123}I-labelled cocaine analogue FP-CIT (DaTscan, GE Healthcare) in patients with AD and dementia with Lewy bodies reported that decreased DAT binding potential values in the putamen correlated with the severity of apathy as measured with the Neuropsychiatric Inventory (David et al., 2008). Based on this study by David et al. the possibility was considered that the impaired motivation seen in $App^{NL\text{-}G\text{-}F/NL\text{-}G\text{-}F}$ mice is associated with decreased DAT levels in the CPu. To clarify this relationship in an animal model, we examined whether $App^{NL\text{-}G\text{-}F/NL\text{-}G\text{-}F}$ mice show lower striatal DAT levels than do C57BL/6J mice.

Subcortical tissues including the CPu were dissected from five $App^{NL\text{-}G\text{-}F/NL\text{-}G\text{-}F}$ mice and five C57BL/6J mice, all at 9 months of age, and DAT levels were determined based on their densitometric intensity using western blot analysis (Fig. 5A). The densitometric intensity of DAT was normalized by that of GAPDH. We found that the intensity of DAT in the subcortical tissues including the CPu in $App^{NL\text{-}G\text{-}F/NL\text{-}G\text{-}F}$ mice was significantly lower than that in C57BL/6J mice (C57BL/6J mice: 1.000 ± 0.032, $App^{NL\text{-}G\text{-}F/NL\text{-}G\text{-}F}$ mice: 0.873 ± 0.016, $p < 0.01$ with Student's *t*-test, Fig. 5B). This result indicated the possibility that the impaired motivation observed in $App^{NL\text{-}G\text{-}F/NL\text{-}G\text{-}F}$ mice is related to decreased levels of DAT in the subcortical tissues including the CPu.

4. Discussion

We employed $App^{NL\text{-}G\text{-}F/NL\text{-}G\text{-}F}$ mice in which Aβ deposition starts at 2 months of age and examined whether persistent increase of Aβ deposition impairs motivation. We found that $App^{NL\text{-}G\text{-}F/NL\text{-}G\text{-}F}$ mice overall do not show an impairment in instrumental motivation from 16 to 39 weeks of age. However, in the group sub analysis of 11 $App^{NL\text{-}G\text{-}F/NL\text{-}G\text{-}F}$ mice, we observed that an increased number of cored amyloid plaques in the CPu coincided with impaired motivation at 39 weeks of age. Furthermore, we found with western blot analysis that $App^{NL\text{-}G\text{-}F/NL\text{-}G\text{-}F}$ mice at 9 months old have decreased DAT levels in the CPu.

The lack of a time-dependent effect on behavior in the testing sessions (Fig. 1C–E) indicated that behavior was not affected when amyloid plaques increased from approximately 4% to approximately 8% in the cortex and from approximately 1% to approximately 3% subcortically (4 months–9 months of age; see Fig. 2b in Saito et al., 2014). However, the comparison among the 11 $App^{NL\text{-}G\text{-}F/NL\text{-}G\text{-}F}$ mice at 39 weeks of age showed that some were motivated and some were not, and it could be considered that there were no differences in the mean break point between $App^{NL\text{-}G\text{-}F/NL\text{-}G\text{-}F}$ and C57BL/6J mice. Some $App^{NL\text{-}G\text{-}F/NL\text{-}G\text{-}F}$ mice showed impaired motivation in tandem with cored amyloid plaque deposition in the CPu; therefore, if $App^{NL\text{-}G\text{-}F/NL\text{-}G\text{-}F}$ mice with extensive cored amyloid plaque deposition in the CPu are employed, our operant testing method may show a significant decrease of the break point in $App^{NL\text{-}G\text{-}F/NL\text{-}G\text{-}F}$ mice compared to C57BL/6J mice.

Cored amyloid plaques are reportedly strongly neurotoxic, which causes synaptic and neuronal loss (D'Andrea and Nagele, 2010; Serrano-Pozo et al., 2011; Urbanc et al., 2002). From our results, it may be proposed that the impaired motivation seen in $App^{NL\text{-}G\text{-}F/NL\text{-}G\text{-}F}$ mice derives from striatal dysfunction due to the neurotoxicity of cored amyloid plaques. The CPu is part of the reward system, and some reports have indicated that striatal dysfunction leads to impaired motivation. A study of ablation targeting the CPu showed loss of motivation in the food-oriented lever-press task (Tsutsui-Kimura et al., 2017). The middle cerebral artery occlusion mouse model, which is a major ischemic mouse model and exhibits partial ischemia of the CPu, also showed impaired motivation in the food-oriented lever-press task (Linden et al., 2015).

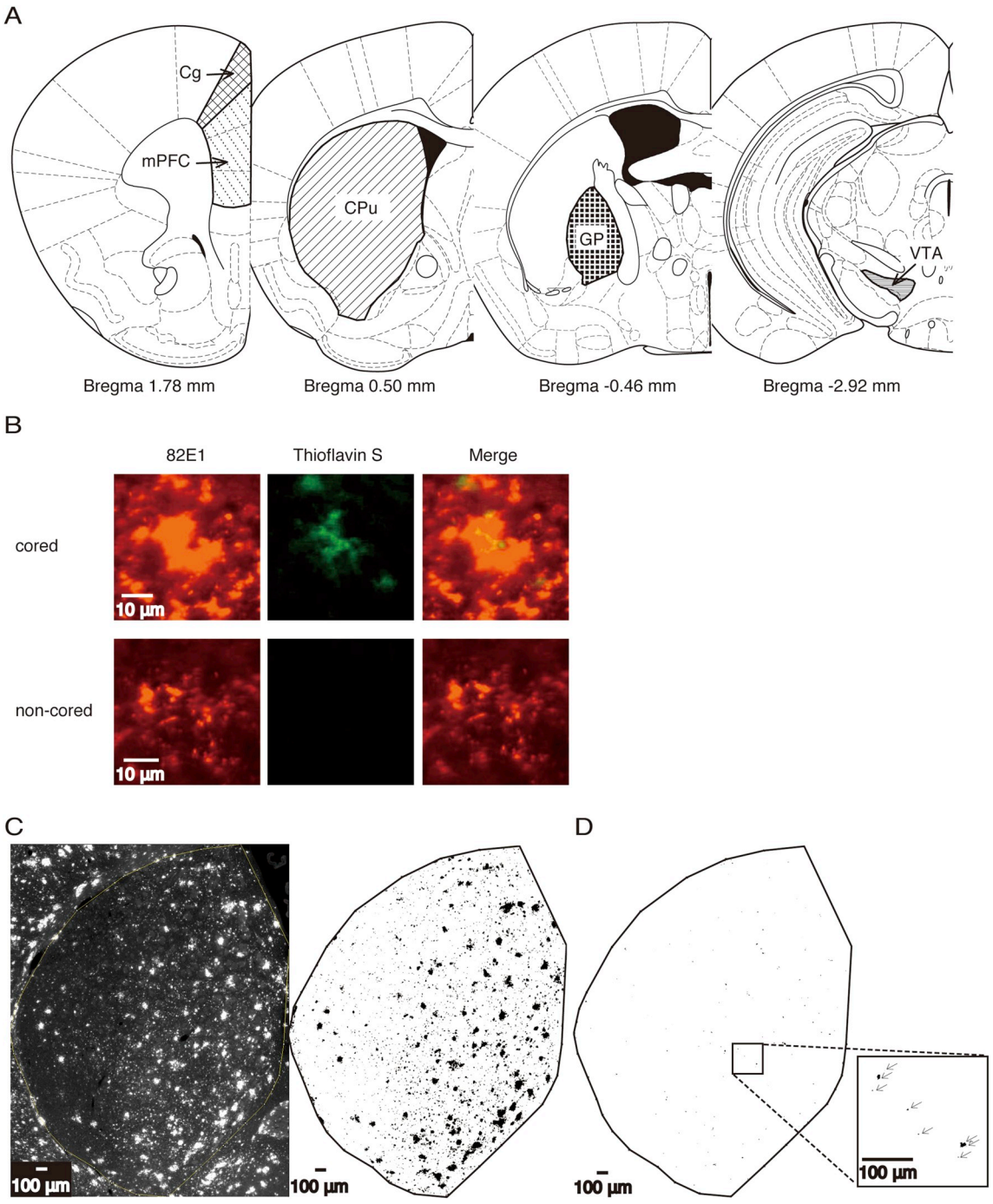

Fig. 3. The histopathological analysis of amyloid plaques in $App^{NL\text{-}G\text{-}F/NL\text{-}G\text{-}F}$ mice at 39 weeks of age. **A,** five analyzed areas related to the reward system are shown. **B,** the image shows double staining with the 82E1 antibody (red) and Thioflavin S (green). The 82E1 antibody staining showed amyloid plaques, and among them, Thioflavin S (+) amyloid plaques are cored (upper row) and Thioflavin S (−) amyloid plaques are non-cored (lower row). **C,** the left image displays the staining of amyloid plaques with the 82E1 antibody in the CPu and the right image displays a binary image analyzed by applying an ImageJ algorithm. **D,** the image displays a binary image of the staining of cored amyloid plaques with Thioflavin S in the CPu analyzed by ImageJ. The arrow in the enlarged image indicates the count of the cored amyloid plaques.
AbbreviationsCg, cingulate cortex; CPu, striatum; GP, globus pallidus; mPFC, medial prefrontal cortex; VTA, ventral tegmental area.

From the results of this study, we propose that cored amyloid plaques damage the DAT in the CPu in $App^{NL\text{-}G\text{-}F/NL\text{-}G\text{-}F}$ mice (Fig. 6). We showed that increase in cored amyloid plaques in the CPu reduces motivation and that $App^{NL\text{-}G\text{-}F/NL\text{-}G\text{-}F}$ mice have decreased DAT levels in the CPu. In addition, David et al. (2008) reported that decrease of the DAT in the CPu leads to impaired motivation. Therefore, we consider that there may be a pathway, involving the DAT, through which cored amyloid plaque deposition impairs motivation (Fig. 6, black dashed arrow). However, we could not evaluate this pathway in this study because the mice used for the western blot analysis were not the same individuals as those employed for the evaluation of motivation. To our knowledge, the relation between deposition of cored amyloid plaques and decrease in DAT has not been previously reported, and further research of this pathway is expected to contribute toward elucidating the mechanism of impaired motivation in patients with AD.

To the best of our knowledge, only one study examined

Table 1
The results of the histopathological analysis of the ROIs in $App^{NL\text{-}G\text{-}F/NL\text{-}G\text{-}F}$ mice at 39 weeks of age.

$App^{NL\text{-}G\text{-}F/NL\text{-}G\text{-}F}$ mouse	BP	Amyloid plaques (%)					Cored amyloid plaques (n/mm^2)				
		Cg	mPFC	CPu	GP	VTA	Cg	mPFC	CPu	GP	VTA
1	32	15.9	13.7	6.6	9.6	6.1	28.5	36.3	39.7	110.2	46.8
2	32	19.4	19.3	6.3	8.6	5.8	42.7	42.5	41.8	84.0	14.1
3	118	16.0	13.6	5.6	8.4	9.4	71.4	68.6	24.7	83.8	34.4
4	118	14.5	15.1	6.2	7.8	5.0	20.6	35.3	35.0	108.0	40.7
5	62	24.0	20.3	10.0	9.1	5.2	54.3	62.3	49.6	101.6	49.5
6	62	26.7	20.7	10.7	10.0	8.5	81.1	47.2	51.5	80.0	11.1
7	95	32.9	23.9	11.9	11.4	6.1	53.6	66.7	39.5	108.6	
8	118	26.0	23.9	7.8	10.8	10.2	16.3	35.3	37.6	38.5	22.4
9	40	15.1	11.3	5.9	11.0	4.8	42.0	98.5	55.2		61.4
10	32	18.4	15.0	7.6	9.4	10.0	102.7	63.1	47.8	86.5	53.4
11	32	10.1	10.2	8.0	8.7	4.2	80.8	68.8	55.5	60.4	29.5

BP, break point; Cg, cingulate cortex; mPFC, medial prefrontal cortex; CPu, striatum; GP, globus pallidus; VTA, ventral tegmental area.

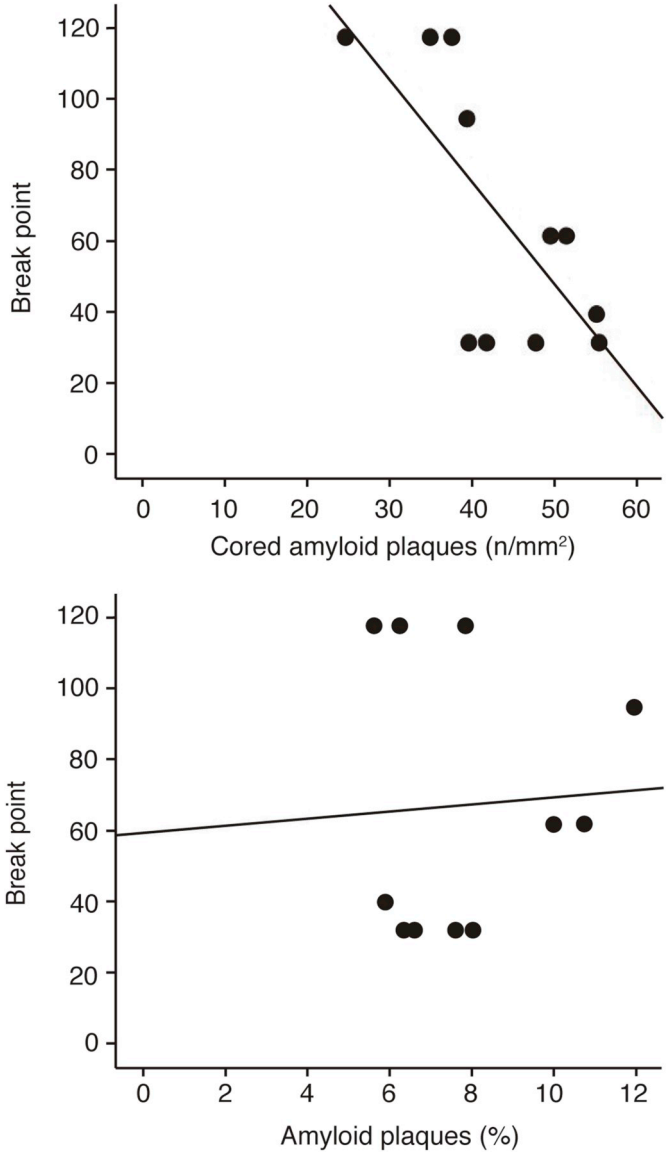

Fig. 4. The result of a stepwise multiple regression analysis with the data of the histopathological analysis of the ROIs and the break point in the 11 $App^{NL\text{-}G\text{-}F/NL\text{-}G\text{-}F}$ mice at 39 weeks of age. **A,** an inverse correlation was found between the number of cored amyloid plaques per mm^2 in the CPu and the break point. **B,** no correlation was found between the %Area of amyloid plaques in the CPu and the break point.
Abbreviations: ROI, region of interest; CPu, striatum.

instrumental motivation by employing a PR reinforcement paradigm (Blackshear et al., 2011) using genetically-modified mice as an AD model. Two of three Tg2576 mice showed impaired motivation at approximately 12 months of age. No histological examination was performed in the study of Tg2576; however, there is a possibility that Tg2576 mice show an association between cored amyloid plaques and motivation in histological analysis, as seen in the $App^{NL\text{-}G\text{-}F/NL\text{-}G\text{-}F}$ mouse.

Aβ43 may be involved in the association between cored amyloid plaques and impaired motivation in the $App^{NL\text{-}G\text{-}F/NL\text{-}G\text{-}F}$ mice at 39 weeks of age. Aβ40 and Aβ42 are the major forms of Aβ, but the longer peptide, Aβ43, is more frequently seen than is Aβ40 in cored amyloid plaques in the brains of patients with AD (Welander et al., 2009). In vitro, Aβ43 shows a higher propensity to aggregate and is more neurotoxic than are Aβ40 and Aβ42 in the PS1-R278I knock-in mouse (Saito et al., 2011). Since the distribution of Aβ43 is consistent with that of the Thioflavin S staining, cored amyloid plaques stained with Thioflavin S in the $App^{NL\text{-}G\text{-}F/NL\text{-}G\text{-}F}$ mice in this study might involve neurotoxicity and, thus, cause impaired motivation.

We suggest that a drug with the ability to reduce cored amyloid plaques may rescue the impaired motivation. In fact, triflusal, a compound with potent anti-inflammatory effects in the central nervous system in vivo, significantly reduces cored amyloid plaque load and rescues the cognitive deficits in Tg2576 mice (Coma et al., 2010). The present treatment strategies targeting Aβ40 and Aβ42 have not been reliably shown to prevent the development of core symptoms in patients with AD. In these circumstances, a treatment targeting cored amyloid plaques of Aβ43, which is more neurotoxic and correlates with neurological deficits, may be a breakthrough treatment.

In clinical applications, imaging of cored amyloid plaques may predict symptoms in patients with AD by visualizing the deposition site of cored amyloid plaques. Based on our results, the deposition of cored amyloid plaques in the CPu may predict impaired motivation, while the deposition in the frontal and parietal cortices may predict cognitive impairment, as shown in a study of an AD mouse model (Ito et al., 2014). To image cored amyloid plaques, [(^{18})F]2-[(2-{(E)-2-[2-(dimethylamino)-1,3-thiazol-5-yl]vinyl}-1,3-benzoxazol-6-yl)oxy]-3-fluoropropan-1-ol (FACT) positron emission tomography (PET) is useful, which shows preferential binding to cored amyloid plaques (Furumoto et al., 2013; Ito et al., 2014). [(^{18})F]FACT PET may also contribute to the evaluation of the efficacy of new drugs targeting cored amyloid plaques.

In conclusion, $App^{NL\text{-}G\text{-}F/NL\text{-}G\text{-}F}$ mice in total did not show a significant decline in motivation compared to C57BL/6J mice, but in the sub analysis, $App^{NL\text{-}G\text{-}F/NL\text{-}G\text{-}F}$ mice showed decline in motivation in correlation with the deposition of cored amyloid plaques in the CPu. Furthermore, based on the western blot analysis, it appears that cored amyloid plaques in the CPu may have impaired the DAT, leading to

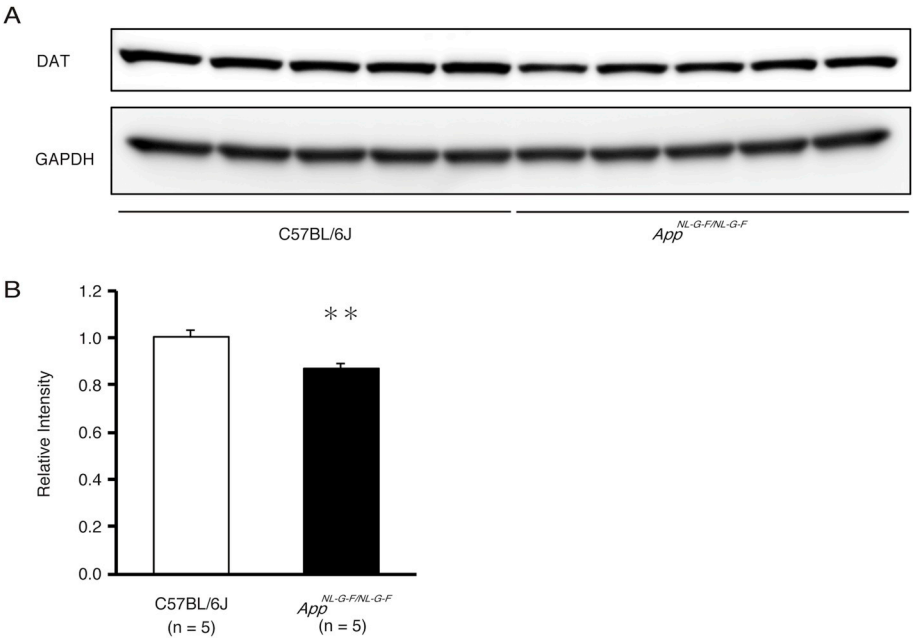

Fig. 5. The results of the western blot analysis used to measure the densitometric intensity of DAT and GAPDH in the subcortical tissues including the CPu in $App^{NL\text{-}G\text{-}F/NL\text{-}G\text{-}F}$ mice and C57BL/6J mice. **A,** antibodies are listed to the left of the panels. **B,** the measured densitometric intensity of DAT was normalized by that of GAPDH. The relative intensity of DAT in $App^{NL\text{-}G\text{-}F/NL\text{-}G\text{-}F}$ mice was significantly lower than that in C57BL/6J mice (Student's *t*-test, $**p < 0.01$).
Abbreviations: DAT, dopamine transporter; CPu, striatum; GAPDH, glyceraldehyde 3-phosphate dehydrogenase.

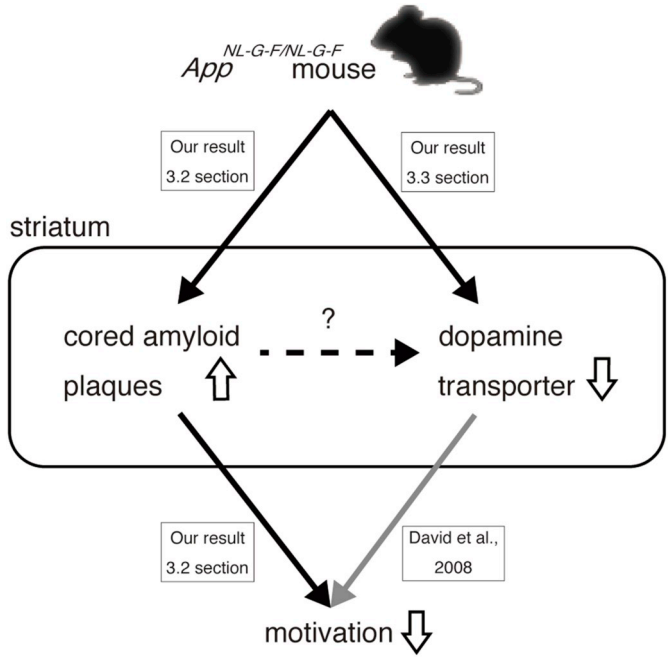

Fig. 6. The potential mechanism causing impaired motivation in $App^{NL\text{-}G\text{-}F/NL\text{-}G\text{-}F}$ mice. Black solid arrows indicate the experimental results of this study and gray solid arrows indicate the findings of a past report. The black dashed arrow is the putative pathway based on the results of this study. The white arrows with the black outline indicate increase and decrease.

impaired motivation. We hope that our results will contribute toward drawing attention to cored amyloid plaques in order to develop a new treatment for impaired motivation in patients with AD.

Acknowledgments

This work was supported by JSPS KAKENHI Grant Number JP16K19321. No competing financial interests exist in connection with this article. The authors would like to thank Naomi Mihira, Marina Tsukamoto, Takashi Manzaki, and Ryusei Kato for technical assistance with the experiments.

References

Benoit, M., Koulibaly, P.M., Migneco, O., Darcourt, J., Pringuey, D.J., Robert, P.H., 2002. Brain perfusion in Alzheimer's disease with and without apathy: a SPECT study with statistical parametric mapping analysis. Psychiatr. Res. 114, 103–111. https://doi.org/10.1016/S0925-4927(02)00003-3.

Blackshear, A.L., Xu, W., Anderson, M., Xu, F., Previti, M.L., Van Nostrand, W.E., Robinson, J.K., 2011. A novel operant testing regimen for multi-construct cognitive characterization of a murine model of Alzheimer's amyloid-related behavioral impairment. Neurobiol. Learn. Mem. 96, 443–451. https://doi.org/10.1016/j.nlm.2011.06.017.

Caravaggio, F., Fervaha, G., Browne, C.J., Gerretsen, P., Remington, G., Graff-Guerrero, A., 2018. Reward motivation in humans and its relationship to dopamine D2/3 receptor availability: a pilot study with dual [11C]-raclopride and [11C]-(+)-PHNO imaging. J. Psychopharmacol. 32, 357–366. https://doi.org/10.1177/0269881118756059.

Coma, M., Sereno, L., Da Rocha-Souto, B., Scotton, T.C., España, J., Sánchez, M.B., Rodríguez, M., Agulló, J., Guardia-Laguarta, C., Garcia-Alloza, M., Borrelli, L.A., 2010. Triflusal reduces dense-core plaque load, associated axonal alterations and inflammatory changes, and rescues cognition in a transgenic mouse model of Alzheimer's disease. Neurobiol. Dis. 38, 482–491. https://doi.org/10.1016/j.nbd.2010.01.019.

Craig, A.H., Cummings, J.L., Fairbanks, L., Itti, L., Miller, B.L., Li, J., Mena, I., 1996. Cerebral blood flow correlates of apathy in Alzheimer disease. Arch. Neurol. 53, 1116–1120. https://doi.org/10.1001/archneur.1996.00550110056012.

D'Andrea, M.R., Nagele, R.G., 2010. Morphologically distinct types of amyloid plaques point the way to a better understanding of Alzheimer's disease pathogenesis. Biotech. Histochem. 85, 133–147. https://doi.org/10.3109/10520290903389445.

David, R., Koulibaly, M., Benoit, M., Garcia, R., Caci, H., Darcourt, J., Robert, P., 2008. Striatal dopamine transporter levels correlate with apathy in neurodegenerative diseases A SPECT study with partial volume effect correction. Clin. Neurol. Neurosurg. 110, 19–24. https://doi.org/10.1016/j.clineuro.2007.08.007.

Eslinger, P.J., Moore, P., Antani, S., Anderson, C., Grossman, M., 2012. Apathy in frontotemporal dementia: behavioral and neuroimaging correlates. Behav. Neurol. 25, 127–136. https://doi.org/10.1155/2012/286427.

Furumoto, S., Okamura, N., Furukawa, K., Tashiro, M., Ishikawa, Y., Sugi, K., Tomita, N., Waragai, M., Harada, R., Tago, T., Iwata, R., 2013. A 18F-labeled BF-227 derivative as a potential radioligand for imaging dense amyloid plaques by positron emission tomography. Mol. Imaging Biol. 15, 497–506. https://doi.org/10.1007/s11307-012-0608-5.

Griffin, W.S.T., Sheng, J.G., Roberts, G.W., Mrak, R.E., 1995. Interleukin-1 expression in different plaque types in Alzheimer's disease: significance in plaque evolution. J. Neuropathol. Exp. Neurol. 54, 276–281. https://doi.org/10.1097/00005072-199503000-00014.

Hamaguchi, T., Tsutsui-Kimura, I., Tanaka, K.F., Mimura, M., 2017. *Yokukansankachimpihange* increased body weight but not food-incentive motivation in wild-type mice. Nagoya J. Med. Sci. 79, 351–362.

Holthoff, V.A., Beuthien-Baumann, B., Kalbe, E., Lüdecke, S., Lenz, O., Zündorf, G., Spirling, S., Schierz, K., Winiecki, P., Sorbi, S., Herholz, K., 2005. Regional cerebral metabolism in early Alzheimer's disease with clinically significant apathy or depression. Biol. Psychiatry 57, 412–421. https://doi.org/10.1016/j.biopsych.2004.11.035.

Ito, H., Shinotoh, H., Shimada, H., Miyoshi, M., Yanai, K., Okamura, N., Takano, H.,

Takahashi, H., Arakawa, R., Kodaka, F., Ono, M., 2014. Imaging of amyloid deposition in human brain using positron emission tomography and [18F]FACT: comparison with [11C]PIB. Eur. J. Nucl. Med. Mol. Imaging 41, 745–754. https://doi.org/10.1007/s00259-013-2620-7.

Kang, J.Y., Lee, J.S., Kang, H., Lee, H.W., Kim, Y.K., Jeon, H.J., Chung, J.K., Lee, M.C., Cho, M.J., Lee, D.S., 2012. Regional cerebral blood flow abnormalities associated with apathy and depression in Alzheimer disease. Alzheimers Dis. Assoc. Disord. 26, 217–224. https://doi.org/10.1097/WAD.0b013e318231e5fc.

Levy, R., Dubois, B., 2006. Apathy and the functional anatomy of the prefrontal cortex-basal ganglia circuits. Cerebr. Cortex 16, 916–928. https://doi.org/10.1093/cercor/bhj043.

Linden, J., Plumier, J.C., Fassotte, L., Ferrara, A., 2015. Focal cerebral ischemia impairs motivation in a progressive FR schedule of reinforcement in mice. Behav. Brain Res. 279, 82–86. https://doi.org/10.1016/j.bbr.2014.10.042.

Marin, R.S., 1990. Differential diagnosis and classification of apathy. Am. J. Psychiatry 147, 22–30. https://doi.org/10.1176/ajp.147.1.22.

Marshall, G.A., Monserratt, L., Harwood, D., Mandelkern, M., Cummings, J.L., Sultzer, D.L., 2007. Positron emission tomography metabolic correlates of apathy in Alzheimer disease. Arch. Neurol. 64, 1015–1020. https://doi.org/10.1001/archneur.64.7.1015.

Masuda, A., Kobayashi, Y., Kogo, N., Saito, T., Saido, T.C., Itohara, S., 2016. Cognitive deficits in single *App* knock-in mouse models. Neurobiol. Learn. Mem. 135, 73–82. https://doi.org/10.1016/j.nlm.2016.07.001.

Mehla, J., Lacoursiere, S.G., Lapointe, V., McNaughton, B.L., Sutherland, R.J., McDonald, R.J., Mohajerani, M.H., 2019. Age-dependent behavioral and biochemical characterization of single APP knock-in mouse ($App^{NL\text{-}G\text{-}F/NL\text{-}G\text{-}F}$) model of Alzheimer's disease. Neurobiol. Aging 75, 25–37. https://doi.org/10.1016/j.neurobiolaging.2018.10.026.

Mori, T., Shimada, H., Shinotoh, H., Hirano, S., Eguchi, Y., Yamada, M., Fukuhara, R., Tanimukai, S., Zhang, M.R., Kuwabara, S., Ueno, S.I., 2014. Apathy correlates with prefrontal amyloid beta deposition in Alzheimer's disease. J. Neurol. Neurosurg. Psychiatry 85, 449–455. https://doi.org/10.1136/jnnp-2013-306110.

Richardson, N.R., Roberts, D.C., 1996. Progressive ratio schedules in drug self-administration studies in rats: a method to evaluate reinforcing efficacy. J. Neurosci. Methods 66, 1–11. https://doi.org/10.1016/0165-0270(95)00153-0.

Robert, P.H., Berr, C., Volteau, M., Bertogliati, C., Benoit, M., Sarazin, M., Legrain, S., Dubois, B., 2006. Apathy in patients with mild cognitive impairment and the risk of developing dementia of Alzheimer's disease: a one-year follow-up study. Clin. Neurol. Neurosurg. 108, 733–736. https://doi.org/10.1016/j.clineuro.2006.02.003.

Saga, Y., Hoshi, E., Tremblay, L., 2017. Roles of multiple globus pallidus territories of monkeys and humans in motivation, cognition and action: an anatomical, physiological and pathophysiological review. Front. Neuroanat. 11, 30. https://doi.org/10.3389/fnana.2017.00030.

Saito, T., Suemoto, T., Brouwers, N., Sleegers, K., Funamoto, S., Mihira, N., Matsuba, Y., Yamada, K., Nilsson, P., Takano, J., Nishimura, M., Iwata, N., Van Broeckhoven, C., Ihara, Y., Saido, T.C., 2011. Potent amyloidogenicity and pathogenicity of Abeta43. Nat. Neurosci. 14, 1023–1032. https://doi.org/10.1038/nn.2858.

Saito, T., Matsuba, Y., Mihira, N., Takano, J., Nilsson, P., Itohara, S., Iwata, N., Saido, T.C., 2014. Single App knock-in mouse models of Alzheimer's disease. Nat. Neurosci. 17, 661–663. https://doi.org/10.1038/nn.3697.

Sasaguri, H., Nilsson, P., Hashimoto, S., Nagata, K., Saito, T., De Strooper, B., Hardy, J., Vassar, R., Winblad, B., Saido, T.C., 2017. APP mouse models for Alzheimer's disease preclinical studies. EMBO J. 36, 2473–2487. https://doi.org/10.15252/embj.201797397.

Schroeter, M.L., Vogt, B., Frisch, S., Becker, G., Seese, A., Barthel, H., Mueller, K., Villringer, A., Sabri, O., 2011. Dissociating behavioral disorders in early dementia-An FDG-PET study. Psychiatr. Res. 194, 235–244. https://doi.org/10.1016/j.pscychresns.2011.06.009.

Serrano-Pozo, A., Frosch, M.P., Masliah, E., Hyman, B.T., 2011. Neuropathological alterations in Alzheimer disease. Cold Spring Harb. Perspect. Med. 1, a006189. https://doi.org/10.1101/cshperspect.a006189.

Sondell, A., Rosendahl, E., Sommar, J.N., Littbrand, H., Lundin-Olsson, L., Lindelöf, N., 2018. Motivation to participate in high-intensity functional exercise compared with a social activity in older people with dementia in nursing homes. PLoS One 13, e0206899. http://doi.org/10.1371/journal.pone.0206899.

Teng, E., Lu, P.H., Cummings, J.L., 2007. Neuropsychiatric symptoms are associated with progression from mild cognitive impairment to Alzheimer's disease. Dement. Geriatr. Cognit. Disord. 24, 253–259. https://doi.org/10.1159/000107100.

Tsutsui-Kimura, I., Takiue, H., Yoshida, K., Xu, M., Yano, R., Ohta, H., Nishida, H., Bouchekioua, Y., Okano, H., Uchigashima, M., Watanabe, M., 2017. Dysfunction of ventrolateral striatal dopamine receptor type 2-expressing medium spiny neurons impairs instrumental motivation. Nat. Commun. 8, 14304. https://doi.org/10.1038/ncomms14304.

Urbanc, B., Cruz, L., Le, R., Sanders, J., Ashe, K.H., Duff, K., Stanley, H.E., Irizarry, M.C., Hyman, B.T., 2002. Neurotoxic effects of thioflavin S-positive amyloid deposits in transgenic mice and Alzheimer's disease. Proc. Natl. Acad. Sci. U.S.A. 99, 13990–13995.

Welander, H., Frånberg, J., Graff, C., Sundström, E., Winblad, B., Tjernberg, L.O., 2009. Abeta43 is more frequent than Abeta40 in amyloid plaque cores from Alzheimer disease brains. J. Neurochem. 110, 697–706. https://doi.org/10.1111/j.1471-4159.2009.06170.x.

Williams, A.K., 2005. Motivation and dementia. Top. Geriatr. Rehabil. 21, 123–126.

Zhao, Q.F., Tan, L., Wang, H.F., Jiang, T., Tan, M.S., Tan, L., Xu, W., Li, J.Q., Wang, J., Lai, T.J., Yu, J.T., 2016. The prevalence of neuropsychiatric symptoms in Alzheimer's disease: systematic review and meta-analysis. J. Affect. Disord. 190, 264–271. https://doi.org/10.1016/j.jad.2015.09.069.